The Annals of Statistics
1993, Vol. 21, No. 3, 1401–1430

GENERALIZED PERMUTATION POLYTOPES AND EXPLORATORY GRAPHICAL METHODS FOR RANKED DATA[1]

BY G. L. THOMPSON

Southern Methodist University

Exploratory graphical methods for fully and partially ranked data are proposed. In fully ranked data, n items are ranked in order of preference by a group of judges. In partially ranked data, the judges do not completely specify their ranking of the n items. The resulting set of frequencies is a function on the symmetric group of permutations if the data is fully ranked, and a function on a coset space of the symmetric group if the data is partially ranked. Because neither the symmetric group nor its coset spaces have a natural linear ordering, traditional graphical methods such as histograms and bar graphs are inappropriate for displaying fully or partially ranked data.

For fully ranked data, frequencies can be plotted naturally on the vertices of a permutation polytope. A permutation polytope is the convex hull of the $n!$ points in $\mathbb{R}^n$ whose coordinates are the permutations of n distinct numbers. The metrics Spearman's ρ and Kendall's τ are easily interpreted on permutation polytopes. For partially ranked data, the concept of a permutation polytope must be generalized to include permutations of nondistinct values. Thus, a *generalized permutation polytope* is defined as the convex hull of the points in $\mathbb{R}^n$ whose coordinates are permutations of n not necessarily distinct values. The frequencies with which partial rankings are chosen can be plotted in a natural way on the vertices of a generalized permutation polytope. Generalized permutation polytopes induce a new extension of Kendall's τ for partially ranked data. Also, the fixed vector version of Spearman's ρ for partially ranked data is easily interpreted on generalized permutation polytopes.

The problem of visualizing data plotted on polytopes in $\mathbb{R}^n$ is addressed by developing the theory needed to define all the faces, especially the three and four dimensional faces, of any generalized permutation polytope. This requires writing a generalized permutation polytope as the intersection of a system of linear equations, and extending results for permutation polytopes to generalized permutation polytopes. The proposed graphical methods is illustrated on five different data sets.

1. Introduction. Exploratory graphical methods are needed to display frequency distributions for fully and partially ranked data. Fully ranked data occur, for example, when a set of judges are each asked to rank n items in order of preference. Each observation is a permutation of n distinct numbers. The resulting set of frequencies is a function on S_n, the symmetric group of n elements. In partially ranked data, the judges are asked for an incomplete

Received October 1991; revised June 1992.
[1]Supported by NSF Grant DMS-90-02914.
AMS 1991 *subject classifications*. Primary 62-09; secondary 52B05, 52B11, 52B15.
Key words and phrases. Partial ranking, permutation polytope, exploratory data analysis, graphics, Kendall's τ.

ranking of n items. A partial ranking can be represented as a permutation of n nondistinct numbers. A set of frequencies of partial rankings is a function on a coset space of S_n. Because neither the elements of S_n, nor the cosets of S_n, have a natural linear ordering, traditional graphical methods such as histograms and bar graphs cannot be used in a reasonable manner to display frequency distributions for full or partial rankings.

In this paper, graphical techniques are developed to display frequency distributions of ranked data by using generalized permutation polytopes. A polytope is the convex hull of a finite set of points in $\mathbb{R}^n$. Yemelichev, Kovalev and Kravtsov (1984), henceforth referred to as YKK, define a permutation polytope as the convex hull of the $n!$ points in $\mathbb{R}^n$ whose coordinates are the permutations of n distinct numbers. We generalize this definition to accommodate partially ranked data and define a *generalized permutation polytope* to be the convex hull of the points in $\mathbb{R}^n$ whose coordinates are the permutations of n (not necessarily distinct) numbers. Then, to display a set of full or partial rankings, the frequencies with which each permutation is chosen are plotted, not on a line as is done with histograms, but on the vertices of the generalized permutation polytope.

The generalized permutation polytope on which the frequencies are displayed is inscribed in a sphere in an $n - 1$ dimensional subspace of $\mathbb{R}^n$. Hence, for $n > 4$, the problem of visualization of points on a polytope in higher dimensions must be addressed. The approach proposed in this paper is to explore higher dimensional polytopes by examining the three dimensional faces and portions of the four dimensional faces. Theorems are proved which characterize all of the faces of any generalized permutation polytope. These theorems depend on first defining a generalized permutation polytope as a solution to a finite set of linear inequalities, and then extending the results of YKK (which are only for permutation polytopes with distinct values) to generalized permutation polytopes. In particular, for any full or partial ranking it is shown that any two-dimensional face is combinatorially equivalent to either a triangle, a square or a hexagon, and any three dimensional face is combinatorially equivalent to one of the following eight Archimedean solids: truncated tetrahedron, triangular prism, octahedron, tetrahedron, truncated octahedron, cube, cuboctahedron or hexagonal prism. For fully ranked data, all two-dimensional faces are combinatorially equivalent to either squares or hexagons, and all three-dimensional faces to either truncated octahedrons, cubes or hexagonal prisms.

The resulting graphical displays for fully ranked data are especially useful as diagnostic tools because the two metrics most commonly used for modeling ranked data, Kendall's τ and Spearman's ρ, have natural geometric interpretations on permutation polytopes. For fully ranked data Kendall's τ is the minimum number of edges that must be traversed to get from one vertex of the permutation polytope to another; and Spearman's ρ is proportional to the straight line distance between vertices. This is closely related to the observation by McCullagh (1993) that the $n!$ elements of S_n lie on the surface of a sphere in $\mathbb{R}^{n-1}$ in such a way as to be compatible with both Kendall's τ and Spearman's ρ. For partial rankings, there are a variety of extensions of

Kendall's τ and Spearman's ρ that have been proposed [cf. Critchlow (1985) or Diaconis (1988)]. On generalized permutation polytopes, the straight line distance between two vertices is proportional to the fixed vector extension of Spearman's ρ. More significantly, the minimum number of edges that must be traversed to get from one vertex to another induces a new and very reasonable extension of Kendall's τ for partially ranked data.

Other graphical methods for representing rankings include multidimensional scaling, minimal spanning trees and nearest neighbor graphs as discussed by Diaconis (1988) for fully ranked data and by Critchlow (1985) for partially ranked data. Cohen (1990) presents additional exploratory data techniques for both full and partial rankings, and Cohen and Mallows (1980) propose graphical procedures based on multidimensional scaling and biplots. Baba (1986, 1988) discusses graphical methods for ranked data that yield tests for concordance.

In Section 2, the proposed graphical techniques are introduced and illustrated for $n = 3$ and $n = 4$ with ordinary full rankings. Section 3 develops the theory needed for the proposed graphical method for $n > 4$ and for partially ranked data with a common set of pseudoranks. This includes characterizing all of the faces of generalized permutation polytopes, and defining the extension of Kendall's τ for partially ranked data as induced by the generalized permutation polytopes. Section 4 illustrates the usefulness of the results in Section 3 by applying them to three data sets with partial rankings and $n > 4$. Section 5 concludes with proofs.

2. Permutation polytopes for fully ranked data with $n = 3, 4$. Before developing the concepts in general, the proposed graphical technique is illustrated with ordinary full rankings for $n = 3$ and $n = 4$. In fully ranked data, a judge can express preferences for n items either as an ordering or as a ranking. Orderings are denoted by permutations of the n item labels, and are often bracketed by $\langle\ \rangle$. Items are frequently labeled with the integers 1 through n, but in this section, items will be labeled with letters to avoid confusion between rankings and orderings. For example, $\langle B, C, A, D\rangle$ means that item B is ranked first, item C second, item A third and item D is ranked last. A ranking is a permutation of n values that are written as a vector $\boldsymbol{\pi} = (\pi_1, \ldots, \pi_n)$, where π_1 is the rank of item A, π_2 is the rank of item B and so on. The ranking corresponding to the ordering $\langle B, C, A, D\rangle$ is (3, 1, 2, 4).

Figure 1 shows how the orderings corresponding to the six elements of S_3 can be placed naturally on a hexagon. Note that two points are adjacent and connected by an edge if their orderings differ by a pairwise adjacent transposition, or equivalently, if their rankings differ by an inversion of two consecutive values. Hence, the minimum number of edges that must be transversed on the hexagon to get from one vertex to another is equal to Kendall's τ. Formally, if $\boldsymbol{\pi}$ and $\boldsymbol{\sigma}$ are two full rankings, then $\tau(\boldsymbol{\pi}, \boldsymbol{\sigma})$ is defined to be the number of pairs (i, j) such that $\pi_i < \pi_j$ and $\sigma_i > \sigma_j$. This is equivalent to the minimum number of pairwise adjacent transpositions needed to change the ordering corresponding to $\boldsymbol{\pi}$ into the ordering corresponding to $\boldsymbol{\sigma}$. The placement of the vertices in Figure 1 is also related to Spearman's ρ which is defined as

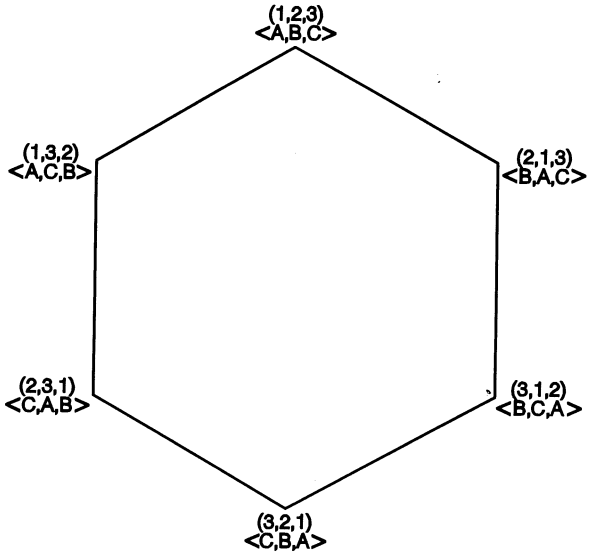

FIG. 1. *Orderings and rankings off* 3 *items on a hexagon.*

$\rho(\boldsymbol{\pi}, \boldsymbol{\sigma}) = (\sum_{i=1}^{n}(\pi_i - \sigma_i)^2)^{1/2}$. If the edges of the regular hexagon are all of length $\sqrt{2}$, then Spearman's ρ is the Euclidean distance between two vertices. Also note that the two vertices of an edge of the hexagon either have the same item ranked first or the same item ranked last.

To illustrate the proposed graphical techniques with $n = 3$, consider the data in Table 1 from Duncan and Brody (1982) in which 1439 people were asked to rank city, suburban and rural living in order of preference. The respondent's current residence is recorded as a classification factor, and within each level, the relative frequencies of each permutation are calculated. In Figures 2a, 2b and 2c these relative frequencies are plotted on the corresponding vertices of three hexagons. The three hexagons correspond to the three levels, and the sizes of the circles at the vertices indicate the relative frequen-

TABLE 1
Data set ($n = 3$ *residence types with a classification factor*; 1439 *survey respondents*)

Orderings	Rankings	Frequencies				Relative frequencies		
		City	Suburb	Rural	Total	City	Suburb	Rural
$\langle C, S, R \rangle$	(1, 2, 3)	210	22	10	242	0.330	0.044	0.033
$\langle C, R, S \rangle$	(1, 3, 2)	23	4	1	28	0.036	0.008	0.003
$\langle S, C, R \rangle$	(2, 1, 3)	111	45	14	170	0.174	0.090	0.046
$\langle S, R, C \rangle$	(3, 1, 2)	204	299	125	628	0.320	0.598	0.414
$\langle R, C, S \rangle$	(2, 3, 1)	8	4	0	12	0.013	0.008	0.000
$\langle R, S, C \rangle$	(3, 2, 1)	81	126	152	359	0.127	0.252	0.503
		637	500	302	1439	1.000	1.000	0.999

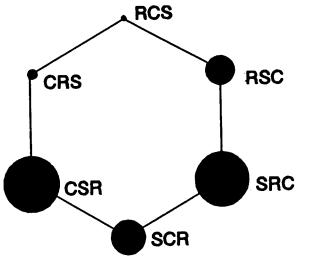

FIG. 2a. *Relative frequencies of city dwellers.*

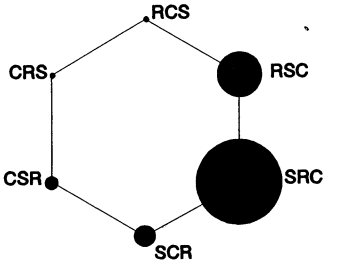

FIG. 2b. *Relative frequencies of suburb dwellers.*

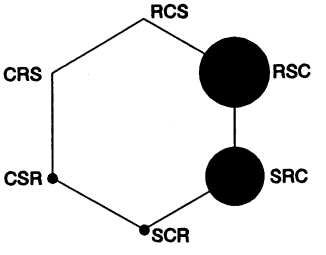

FIG. 2c. *Relative frequencies of rural dwellers.*

cies. It is immediately obvious that rural and suburban residents have similar preferences to each other, and both are different from city dwellers. Those who prefer the city as their first choice seem to live in the city. A relatively small percentage of rural and suburban dwellers prefer their current location least, while a much larger percentage of city dwellers would rather be anyplace else. In the case of $n = 3$, the proposed graphics are similar to the plots of Cohen and Mallows (1980) in which circles with areas proportional to the frequencies are placed at the ends of six vectors radiating from the origin.

These ideas [see, e.g., Knuth (1981), McCullagh (1993) and Thompson (1993)] can be extended to $n = 4$ by placing the 24 permutations at the vertices of a truncated octahedron, as shown in Figure 3. The truncated octahedron is an Archimedean solid with eight hexagonal faces and six square faces. In Figure 3, as in Figure 1, τ is the minimum number of edges that

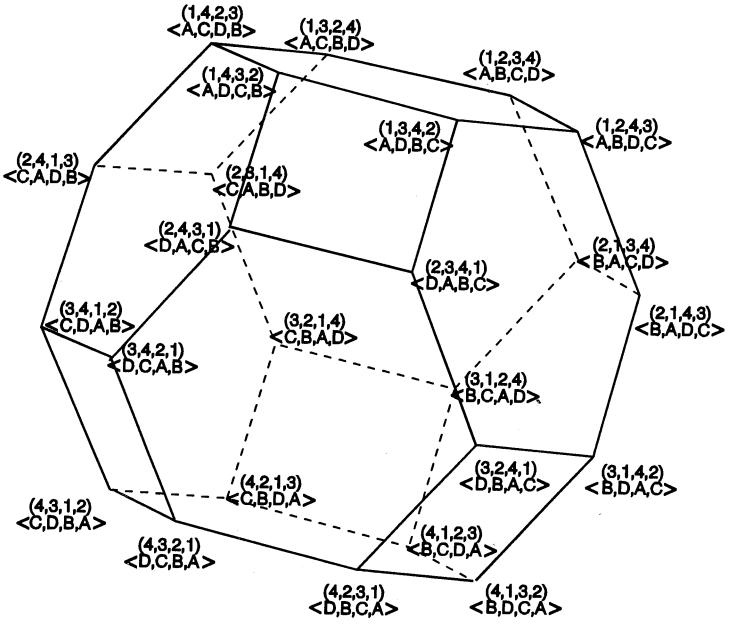

FIG. 3. *Orderings and rankings of* 4 *items on a truncated octahedron.*

must be traversed to get from one vertex to another, and ρ is the Euclidian distance between two vertices if each edge is of length $\sqrt{2}$ [see Schulman (1979) for a discussion]. Examination of the two-dimensional faces of the truncated octahedron in Figure 3 shows that the four vertices of any square have the same two items ranked in the first two positions and the remaining two items ranked in the last two positions. Similarly, the six vertices on any hexagon all have either the same item ranked first or the same item ranked last. There are 36 one-dimensional faces which are edges. The two vertices of any edge agree on the ranking of the first and last choice if the edge is between two hexagons, and the vertices agree on either the first two choices or the last two choices if the edge is between a square and a hexagon. This idea that each face of a permutational polytope has a "defining property" is instrumental in the development of the proposed graphical methods for $n > 4$.

To illustrate the effectiveness of plotting fully ranked data with $n = 4$ on truncated octahedrons, consider the following example. At the beginning of a course in literary criticism, 38 high school students read the short story by Faulkner and ranked four different styles of literary criticism in order of their preference. At the conclusion of the course, they read another short story by Faulkner and again ranked the same four styles of literary criticism. The four styles were authorial (a), comparative (c), personal (p) and textural (t); and the question of interest was whether or not the post-course rankings had moved in the direction of the teacher's own preferred ordering $\langle p, c, a, t \rangle$. Table 2 contains the pre- and post-course rankings. The frequencies of the 38 pre-course rankings are shown in Figure 4a and the 38 post-course rankings

TABLE 2
Data set (n = 4 types of literary criticism, 38 students)

Ordering	Frequencies	
	Before	**After**
ACPT	0	0
ACTP	0	1
ATCP	0	0
ATPC	0	1
APTC	4	1
APCT	1	0
CAPT	0	1
CATP	0	2
CTPA	2	3
CTAP	1	4
CPAT	1	5
CPTA	1	4
PCAT	3	2
PCTA	2	4
PTAC	2	0
PTCA	2	2
PATC	2	2
PACT	3	1
TACP	1	1
TAPC	0	0
TCPA	4	2
TCAP	2	0
TPAC	2	0
TPCA	5	2

Teacher's preference: PCAT.

are shown in Figure 4b. Although the bivariate nature of the data is lost, valuable insight into this data is gained from the plots. Most obviously, the frequencies do change a great deal between the two sets of rankings. First, there seems to be a notable increase in the frequencies at the vertices of the hexagon corresponding to the six orderings that begin with c. The post-course rankings do not seem to have moved *toward* the teacher's preferred ranking, $\langle p, c, a, t \rangle$, but as suggested by the conclusions of Critchlow and Verducci (1989), they appear to be *closer to* $\langle p, c, a, t \rangle$ than are the pre-course rankings. One might hypothesize that the orderings have moved toward $\langle c, p, t, a \rangle$ because almost half of the post-rankings lie either on $\langle c, p, t, a \rangle$ or on one of the three vertices within one edge (pairwise transposition) of $\langle c, p, t, a \rangle$. McCullagh and Ye (1993) reach a similar conclusion which they illustrate by plotting the vectors of the average pre- and post-course ranking on a truncated octahedron. Other observations that can be drawn from Figure 4 include the following:

1. The frequencies at the six vertices corresponding to the ordering that end in c decrease.

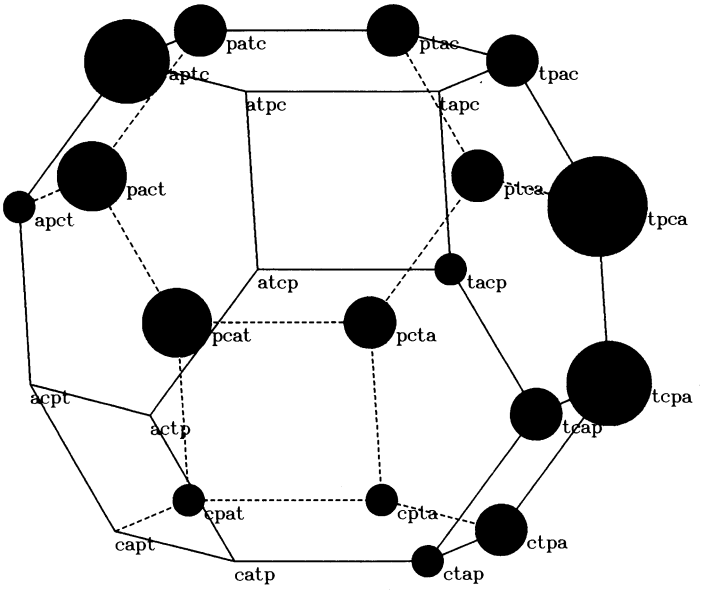

FIG. 4a. *Literary criticism data—before.*

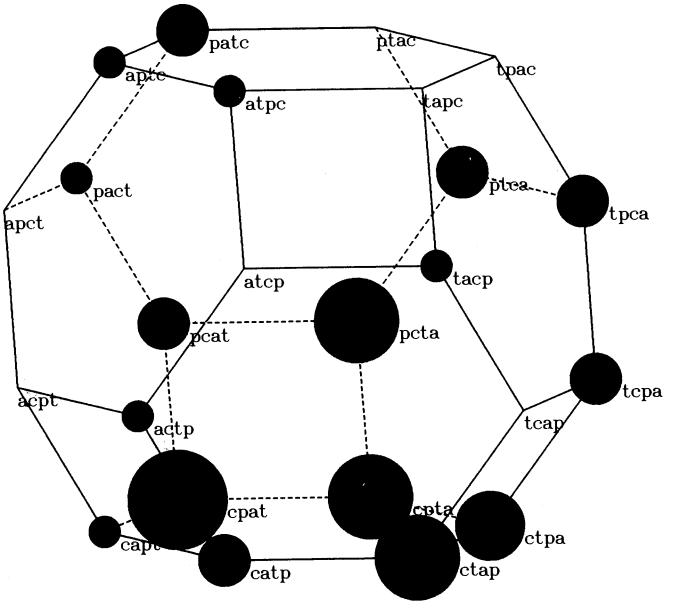

FIG. 4b. *Literary criticism data—after.*

2. Style a is rarely chosen as either a first or second choice after the course is completed.
3. The incidence of style t as a first choice decreases.

To make the plots perceptually accurate, the areas of the circles in Figures 2 and 4 are based on Steven's law which says that a person's perceived scale p of the size of an area is

$$p \propto (\text{area})^{0.7}$$

[Cleveland (1985)]. Hence, the areas of the circles are calculated as

$$\text{area} \propto f^{10/7},$$

where f is the value of the frequency. If the area is proportional to the frequency, area $\propto f$, then small circles appear too large and large circles appear too small. Conversely, if the radius of the circle is proportional to the frequency so that area $\propto f^2$, then large values are magnified and small values are minimized.

3. Permutation polytopes with arbitrary pseudoranks. To most easily extend the ideas in Section 2 to partially ranked data and to rankings of more than four items, we will first define ranked data in terms of pseudoranks. With pseudoranks, a full or partial ranking is a vector whose elements are a permutation of n not necessarily distinct numbers, $0 < a_1 \le a_2 \le \cdots \le a_n$. Ordinary ranks correspond to $a_i = i$. In partially ranked data, the n items are partitioned into r groups of sizes $n_1, n_2, \ldots, n_r$ such that $\sum_{i=1}^{r} n_i = n$. The judges' preferences are then specified as rankings via the pseudoranks

$$(1) \qquad \begin{aligned} 0 < a_1 = \cdots = a_{n_1} < a_{n_1+1} = \cdots = a_{n_1+n_2} < \cdots < a_{n-n_r+1} \\ = \cdots = a_n. \end{aligned}$$

Fully ranked data corresponds to $r = n$ and $n_1 = n_2 = \cdots = n_r = 1$. Note that there are $\binom{n}{n_1 \; n_2 \; n_3 \; \cdots \; n_r}$ distinct permutations of the pseudoranks. It should be noted that the proposed graphical methods only apply to data sets in which all of the partial rankings are permutations of the same set of pseudoranks.

With pseudoranks, an ordering is a permutation of the item labels such that the first item is assigned the smallest pseudorank and so on, and the last item is assigned the largest pseudorank. To denote partial orderings we will adopt the notation of Crichlow (1985) in which the n_i items in the ith group are enclosed in parentheses. Thus, $\langle a, (b, c), d \rangle$ means that a is ranked first, d is ranked last and no distinction is made between b and c.

To plot fully or partially ranked data with arbitrary pseudoranks, first consider the $\binom{n}{n_1 \; n_2 \; n_3 \; \cdots \; n_r}$ permutations of $0 < a_1 \le a_2 \le \cdots \le a_n$ as points in $\mathbb{R}^n$. A generalized permutation polytope is defined as the convex hull of these points. As in Section 2, a set of ranked data can be graphed on the resulting polytope by placing circles whose radii are determined by

$$\text{radius} \propto f^{5/7}$$

at each appropriate vertices. The visual impact of other methods of displaying the frequencies at the vertices merits further study. For example, the magnitude of the frequencies could be indicated, not by the size of the circles, but by color, gray scale shading or pattern.

The resulting polytope in $\mathbb{R}^n$ lies in the intersection of the sphere

$$\sum_{i=1}^{n} (x_i - \bar{a})^2 = \sum_{i=1}^{n} (a_i - \bar{a})^2$$

and the $n - 1$ dimensional hyperplane

$$\sum_{i=1}^{n} x_i = n\bar{a},$$

where $\bar{a} = n^{-1}\Sigma_{i=1}^{n} a_i$. The polytope can be mapped into $\mathbb{R}^{n-1}$ by shifting $\Sigma_{i=1}^{n} x_i = n\bar{a}$ to $\Sigma_{i=1}^{n} x_i = 0$ and then mapping the hyperplane $\Sigma_{i=1}^{n} x_i = 0$ onto $x_n = 0$ via a transformation equivalent to the Helmert transformation. Because this transformation is orthonormal, Euclidian distances and angles are preserved and the polytope is still inscribed in a sphere in $\mathbb{R}^{n-1}$. For example, as shown in Figure 5, the permutation polytope generated by $a_i = i$, $i = 1, 2, 3$, is a regular hexagon (plus its interior). It is inscribed in a circle contained in the plane $x_1 + x_2 + x_3 = 6$. Figure 5 also shows that if $a_3 = a_2 = 2.5$ and $a_1 = 1$, then the generalized permutation polytope is a triangle in the same plane. Straightforward computations also show that the truncated octahedron discussed in Section 2 is exactly the permutation polytope obtained for fully ranked data with $a_i = i$, $i = 1, 2, 3, 4$.

Because the generalized permutation polytope is difficult to visualize for $n > 4$, we will characterize all of the i-dimensional faces (i-faces) of the polytope for $0 \le i \le n - 2$, and then focus on the special characteristics of the three- and four-dimensional faces. Characterization of all of the faces requires writing a generalized permutation polytope as the solution to a system of linear inequalities. Let N_n be the set $\{1, 2, \ldots, n\}$. YKK [(1984), Chapter 5, Theorem 3.1] show that a permutation polytope can be defined equivalently as the intersection of the following system of linear inequalities:

$$\sum_{i \in \omega} x_i \le \sum_{i=1}^{|\omega|} a_{n+1-i} \quad \text{for all } \omega \subseteq N_n, \tag{2}$$

$$\sum_{i=1}^{n} x_i = \sum_{i=1}^{n} a_i. \tag{3}$$

Although YKK define permutation polytopes only for distinct values (i.e., distinct pseudoranks), their proof of this equivalence does not require the pseudoranks to be distinct. Also, YKK use decreasing values (i.e., $0 < a_n < a_{n-1} < \cdots < a_1$), but without loss of generality we will use nondecreasing values because they are more natural in the context of rankings. The above definition is illustrated in Figure 6. If $a_i = i$, $i = 1, 2, 3$, then (2) and (3) are $x_1 \le 3$, $x_2 \le 3$, $x_3 \le 3$, $x_1 + x_2 \le 5$, $x_1 + x_3 \le 5$, $x_2 + x_3 \le 5$, $x_1 + x_2 + x_3 = 6$. If $a_3 = a_2 = 2.5$ and $a_1 = 1$, then (2) and (3) are $x_1 \le 2.5$, $x_2 \le 2.5$, $x_3 \le 2.5$, $x_1 + x_2 \le 5$, $x_1 + x_3 \le 5$, $x_2 + x_3 \le 5$, $x_1 + x_2 + x_3 = 6$. Note that not all of the equations are needed to define the triangle.

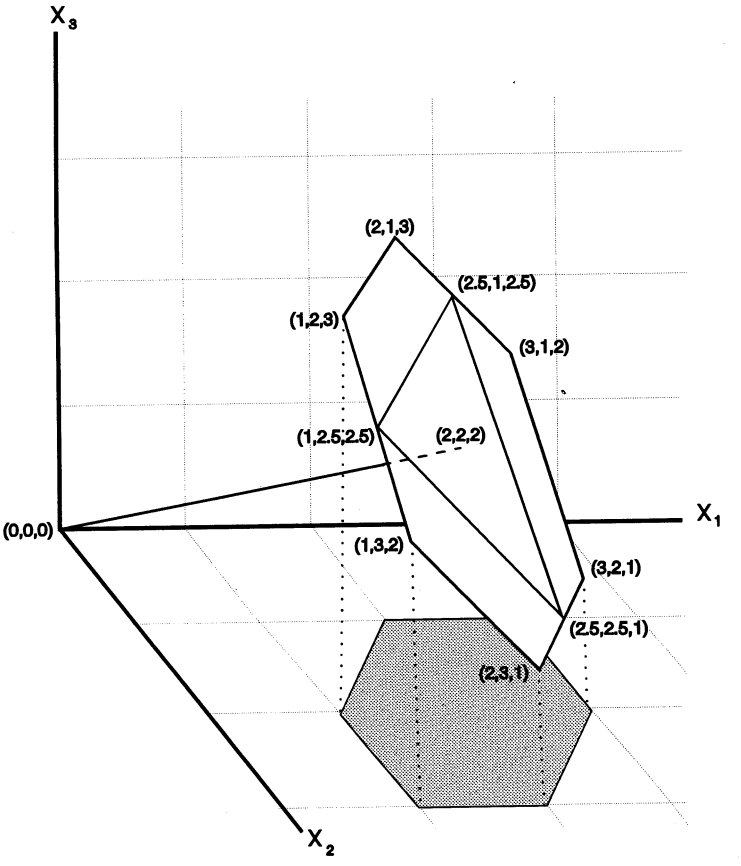

FIG. 5. *Permutation polytopes in* $\mathbb{R}^3$.

In Theorem 3.4 of Chapter 5 YKK characterize all of the faces of a permutation polytope for distinct $0 < a_1 < a_2 < \cdots < a_n$. To characterize the faces of a generalized permutation polytope, we extend their results to nondistinct pseudoranks. The proof of Theorem 1 is in Section 5.

THEOREM 1. *For* $0 \le i \le n-2$, *let* $\omega_1, \ldots, \omega_{n-i-1}$ *be nonempty subsets of* N_n, *let* $\omega_0 = \varnothing$, *and let* $\omega_{n-i} = N_n$. *Then any set of solutions to*

$$\sum_{j\in\omega} x_j \le \sum_{j=1}^{|\omega|} a_{n-j+1} \quad \text{for all } \omega \subseteq N_n, \tag{4}$$

$$\sum_{j\in\omega_k} x_j = \sum_{j=1}^{|\omega_k|} a_{n-j+1} \quad \text{for } k = 1, 2, \ldots, n-i \tag{5}$$

is an i-face of the permutation polytope if and only if

(i) $\omega_1 \subset \omega_2 \subset \cdots \subset \omega_{n-i-1} \subset \omega_{n-i} = N_n$, *and*
(ii) *if* $|\omega_j \Delta \omega_{j-1}| \ge 2$, *then* $a_{n-|\omega_{j-1}|} > a_{n-|\omega_j|+1}$.

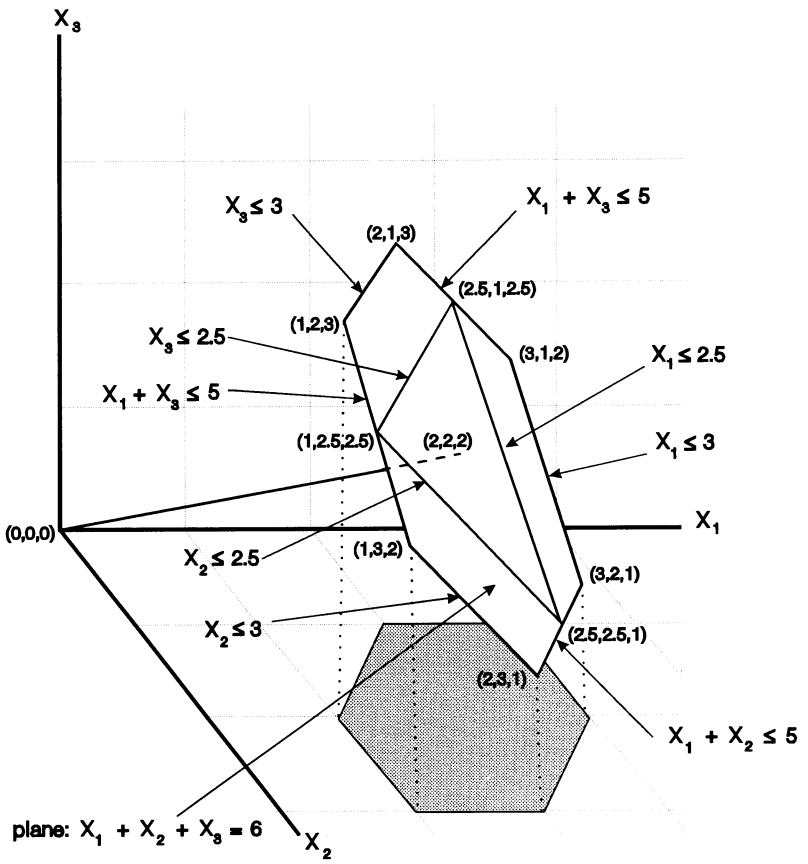

FIG. 6. *Linear constraints for permutation polytopes in* $\mathbb{R}^3$.

The major difference between Theorem 1 and the corresponding Theorem 3.4 in Chapter 5 of YKK is the inclusion of the second condition, namely, if $|\omega_j \Delta \omega_{j-1}| \geq 2$, then $a_{n-|\omega_{j-1}|} > a_{n-|\omega_j|+1}$. This condition is satisfied trivially if all the pseudoranks are distinct. If this condition is omitted with nondistinct pseudoranks, then the resulting set of solutions is a face of the polytope, but its dimension may be less than i. By defining $Q_k = \omega_k \setminus \omega_{k-1}$ and $j_k = |\omega_{k-1}| + 1$ for $1 \leq k \leq n - i$, Theorem 1 can be rephrased more usefully as follows.

THEOREM 1A. *Under the assumptions of Theorem* 1 *it follows that any set of solutions to* (4) *and to*

$$\sum_{j \in Q_k} x_j = \sum_{j=j_k}^{j_{k+1}-1} a_{n-j+1} \quad \text{for } k = 1, 2, \ldots, n - i \tag{6}$$

is an i-face of a generalized permutation polytope if and only if:

(i) $Q_1, Q_2, \ldots, Q_{n-i}$ *are disjoint with* $\bigcup_{j=1}^{n-i} Q_j = N_n$, *and*
(ii) *if* $|Q_j| \geq 2$, *then* $a_{n-|\omega_j|+1} < a_{n-|\omega_{j-1}|}$.

Using the sets Q_k, $1 \leq k \leq n$, Corollary 2 characterizes i-faces in terms of orderings instead of rankings. The proof is in Section 5.

COROLLARY 2. *The set of vertices of an i-face corresponding to a partition* $Q_1, Q_2, \ldots, Q_{n-i}$ *of* $\{1, 2, \ldots, n\}$ *correspond exactly to the orderings* $\langle \pi_n, \pi_{n-1}, \ldots, \pi_1 \rangle$ *(with parentheses inserted in the required places) such that* $Q_k = \{\pi_{j_k}, \pi_{j_k+1}, \ldots, \pi_{j_{k+1}-1}\}$, $k = 1, \ldots, n-i$.

Theorem 1A and Corollary 2 can be used to determine all of the 0-faces (i.e., vertices) of a polytope. For any 0-face, each of the n sets Q_k, $1 \leq k \leq n$, contains exactly one element which induces a permutation $\boldsymbol{\pi} = (\pi_1, \pi_2, \ldots, \pi_n)$ defined by $Q_k = \{\pi_k\}$. Then, (4) and (6) reduce to $x_{\pi_k} = a_{n-k+1}$, and the corresponding ordering, with items labeled with numbers, is obtained by inserting parentheses into $\langle \pi_n, \pi_{n-1}, \ldots, \pi_1 \rangle$ as dictated by the values of n_i, $1 \leq i \leq r$. And the vertices of the generalized permutation polytope are exactly the $\binom{n}{n_1 \; n_2 \; n_3 \; \cdots \; n_r}$ points whose elements are the distinct permutations of the pseudoranks.

For any 1-face, Theorem 1 implies that there is an integer $j \in \{1, 2, \ldots, n\}$ and a permutation $\boldsymbol{\pi}$ such that $Q_k = \{\pi_k\}$, $1 \leq k < j$; $Q_j = \{\pi_j, \pi_{j+1}\}$, $Q_k = \{\pi_{k+1}\}$, $j < k \leq n-1$; and $a_{n-j+1} > a_{n-j}$. Note that $|\omega_{j-1}| = j - 1$ and $|\omega_j| = j + 1$. By Corollary 2, it follows that two vertices of a permutation polytope are adjacent (on the same 1-face) if and only if the orderings, $\langle \pi_n, \pi_{n-1}, \ldots, \pi_{n-j+2}, \pi_{n-j}, \pi_{n-j+1}, \pi_{n-j-1}, \pi_{n-j-2}, \ldots, \pi_1 \rangle$ and $\langle \pi_n, \pi_{n-1}, \ldots, \pi_1 \rangle$ (with parentheses inserted as needed) differ only by the transposition of items π_{n-j} and π_{n-j+1} which do not have the same pseudorank. Equivalently, they are adjacent if they differ by a single inversion of a_k and a_{k+1}, for some $1 \leq k \leq r-1$, where $a_k < a_{k+1}$. This characterization of adjacent points extends Corollary 3.9, Section 5 of YKK to nondistinct values.

Next, Corollary 2 is used to characterize all of the possible the 2-faces of permutation polytopes, as well as identifying all of the possible generalized permutation polytopes for $n = 3$. For any 2-face, there exists a permutation $\boldsymbol{\pi}$ of the n item labels such that one of the three cases in Table 3 holds. Case 1 is combinatorially equivalent to a hexagon because $n - 3$ of the pseudoranks are assigned to $n - 3$ of the items, and the other three pseudoranks, which are distinct, are permuted among the remaining three items. Case 2 is combinatorially equivalent to a triangle because $n - 3$ of the pseudoranks are fixed, and the remaining three pseudoranks, two of which are equal, are permuted among the remaining three items. And case 3 is combinatorially equivalent to a square: $n - 4$ of the pseudoranks are fixed, and of the remaining four pseudoranks, the two smaller are permuted and the two larger are permuted. With squares, it is allowable that $j = i - 1$, and also that $a_{n-j} = a_{n-i}$. Note that

TABLE 3
2-Faces of permutation polytopes

1. $Q_k = \{\pi_k\}, 1 \le k < j$ $Q_j = \{\pi_j, \pi_{j+1}, \pi_{j+2}\}$ $Q_k = \{\pi_{k+2}\}, j < k \le n-2$	$a_{n-j+1} > a_{n-j} > a_{n-j-1}$	Hexagon
2. $Q_k = \{\pi_k\}, 1 \ne k < j$ $Q_j = \{\pi_j, \pi_{j+1}, \pi_{j+2}\}$ $Q_k = \{\pi_{k+2}\}, j < k \le n-2$	$a_{n-j+1} = a_{n-j} > a_{n-j-1}$ or $a_{n-j+1} > a_{n-j} = a_{n-j-1}$	Triangle
3. $Q_k = \{\pi_k\}, 1 \le k < j$ $Q_j = \{\pi_j, \pi_{j+1}\}$ $Q_k = \{\pi_{k+1}\}, j < k < i$ $Q_i = \{\pi_{i+1}, \pi_{i+2}\}$ $Q_k = \{\pi_{k+3}\}, i < k \le n-2$	$a_{n-j+1} > a_{n-j}$ and $a_{n-i} > a_{n-i-1}$	Square

TABLE 4
3-Faces of permutation polytopes

1. $Q_k = \{\pi_k\}, 1 \le k < j$ $Q_j = \{\pi_j, \pi_{j+1}, \pi_{j+2}, \pi_{j+3}\}$ $Q_k = \{\pi_{k+3}\}, j < k \le n-3$	$a_{n-j+1} < a_{n-j} < a_{n-j-1} < a_{n-j-2}$	Truncated octahedron
2. $Q_k = \{\pi_k\}, 1 \le k < j$ $Q_j = \{\pi_j, \pi_{j+1}, \pi_{j+2}, \pi_{j+3}\}$ $Q_k = \{\pi_{k+3}\}, j < k \le n-3$	$a_{n-j+1} = a_{n-j} < a_{n-j-1} < a_{n-j-2}$ or $a_{n-j+1} < a_{n-j} < a_{n-j-1} = a_{n-j-2}$	Truncated tetrahedron
3. $Q_k = \{\pi_k\}, 1 \le k < j$ $Q_j = \{\pi_j, \pi_{j+1}, \pi_{j+2}, \pi_{j+3}\}$ $Q_k = \{\pi_{k+3}\}, j < k \le n-3$	$a_{n-j+1} < a_{n-j} = a_{n-j-1} < a_{n-j-2}$	Cuboctahedron
4. $Q_k = \{\pi_k\}, 1 \le k < j$ $Q_j = \{\pi_j, \pi_{j+1}, \pi_{j+2}, \pi_{j+3}\}$ $Q_k = \{\pi_{k+3}\}, j < k \le n-3$	$a_{n-j+1} = a_{n-j} = a_{n-j-1} < a_{n-j-2}$ or $a_{an-j+1} < a_{n-j} = a_{n-j-1} = a_{n-j-2}$	Tetrahedron
5. $Q_k = \{\pi_k\}, 1 \le k < j$ $Q_j = \{\pi_j, \pi_{j+1}, \pi_{j+2}, \pi_{j+3}\}$ $Q_k = \{\pi_{k+3}\}, j < k \le n-3$	$a_{n-j+1} = a_{n-j} < a_{n-j-1} = a_{n-j-2}$ or $a_{n-j+1} = a_{n-j} < a_{n-j-1} = a_{n-j-2}$	Octahedron
6. $Q_k = \{\pi_k\}, 1 \le k < j$ $Q_j = \{\pi_j, \pi_{j+1}\}$ $Q_k = \{\pi_{k+1}\}, j < k < i$ $Q_i = \{\pi_{i+1}, \pi_{i+2}, \pi_{i+3}\}$ $Q_k = \{\pi_{k+4}\}, i < k \le n-3$	$a_{n-j+1} < a_{n-j}$ and $a_{n-i} < a_{n-i-1} < a_{n-i-2}$	Hexagonal prism
7. $Q_k = \{\pi_k\}, 1 \le k < j$ $Q_j = \{\pi_j, \pi_{j+1}\}$ $Q_k = \{\pi_{k+1}\}, j < k < i$ $Q_i = \{\pi_{i+1}, \pi_{i+2}, \pi_{i+3}\},$ $Q_k = \{\pi_{k+3}\}, i < k \le n-3$	$a_{n-j+1} < a_{n-j}$, and $a_{n-i} < a_{n-i-1} = a_{n-i-2}$ or $a_{n-i} = a_{n-i-1} < a_{n-i-2}$	Triangular prism
8. $Q_k = \{\pi_k\}, 1 \le k < j$ $Q_j = \{\pi_j, \pi_{j+1}\}$ $Q_k = \{\pi_{k+1}\}, j < k < i$ $Q_i = \{\pi_{i+1}, \pi_{i+2}\}$ $Q_k = \{\pi_{k+2}\}, i < k < m$ $Q_m = \{\pi_{m+2}, \pi_{m+3}\}$ $Q_k = \{\pi_{k+3}\}, j < k \le n-3$	$a_{n-j+1} < a_{n-j}$ and $a_{n-i} < a_{n-i-1}$ and $a_{n-m-1} < a_{n-m-2}$	Cube

squares require that $n \geq 4$. If $n = 3$ and if the three pseudoranks are distinct, then the permutation polytope is combinatorially equivalent to a hexagon. Unless it is a regular hexagon, the three short sides alternate with three long sides. If $n = 3$ and two of the pseudoranks are equal (i.e., either just the first choice or just the last choice is specified), then the polytope is an equilateral triangle.

All of the 3-faces of any generalized permutation polytope can be similarly characterized. Clearly, any 3-face is combinatorially equivalent to an Archimedean solid whose 2-faces are triangles, squares, and/or hexagons. For any 3-face, there exists a permutation π of the n item labels such that one of the eight cases shown in Table 4 holds. If the data is fully ranked, then the only possible 3-faces are combinatorially equivalent to truncated octahedrons, hexagonal prisms or cubes. Triangular prisms and hexagonal prisms require that $n \geq 5$, and cubes require that $n \geq 6$. Triangular prisms and hexagonal prisms can also occur when Q_i has two elements and Q_j has three elements with $i > j$.

When $n = 4$ and the four pseudoranks are distinct, that is, when the data is fully ranked, then the polytope is combinatorially equivalent to a truncated octahedron. If $a_i = i$ (i.e., ordinary ranks), the resulting polytope, when mapped into $\mathbb{R}^3$, is the regular truncated octahedron shown in Figure 2. In addition to the truncated octahedron, there are four generalized permutation polytopes for $n = 4$ which correspond to the partial rankings. If $a_1 < a_2 < a_3 = a_4$ or $a_1 = a_2 < a_3 < a_4$, then the generalized permutation polytope is combinatorially equivalent to the truncated tetrahedron shown in Figure 7. Each of the four triangular faces corresponds to the partial rankings in which the same item is ranked first; each of the four hexagonal faces correspond to the partial rankings in which the same item is ranked last. Next, suppose that

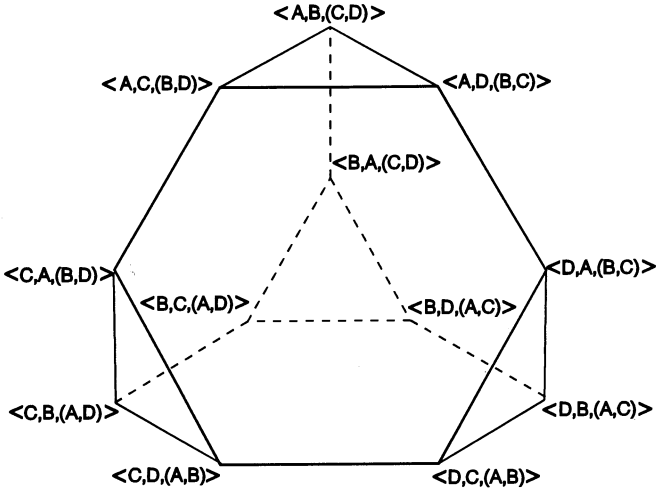

FIG. 7. *Truncated tetrahedron.*

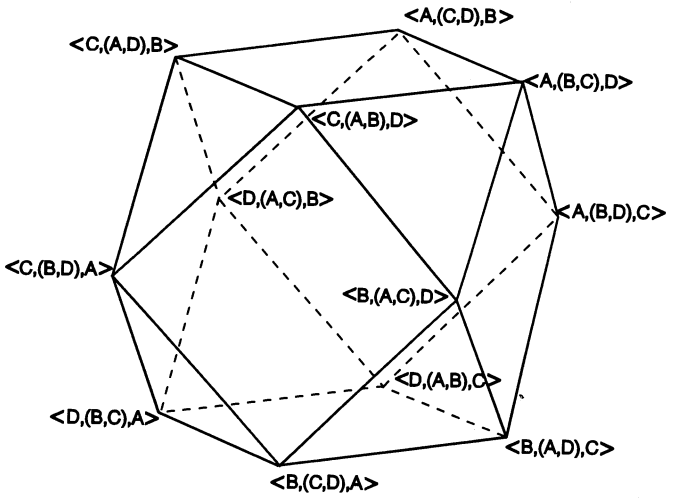

FIG. 8. *Cuboctahedron.*

the only first and last choices are specified so that the pseudoranks are $a_1 < a_2 = a_3 < a_4$. The resulting polytope has 12 vertices and is combinatorially equivalent to the cuboctahedron in Figure 8. If only the first choice or the last choice is specified so that three of the four pseudoranks are equal, then the resulting polytope is a regular tetrahedron (see Figure 9). And lastly, if $n_1 = n_2 = 2$ so that $a_1 = a_2 < a_3 = a_4$, then the permutation polytope is a regular octahedron shown in Figure 10.

Having characterized all of the 0-, 1-, 2- and 3-faces of generalized permutation polytopes, it is of interest to examine the extensions of the metrics Kendall's τ and Spearman's ρ to pseudoranks. First, to extend Spearman's ρ to pseudoranks, denote any two rankings by a_π and a_σ where $\pi = (\pi_1, \ldots, \pi_n)$

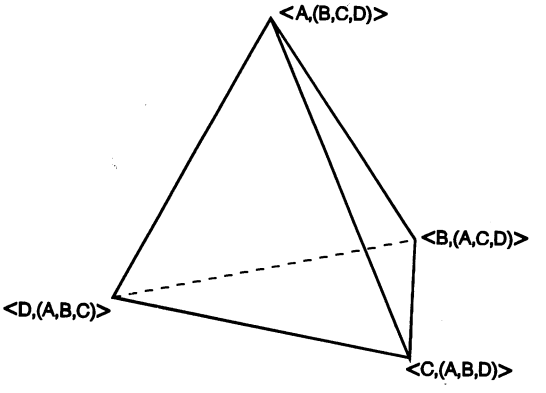

FIG. 9. *Tetrahedron.*

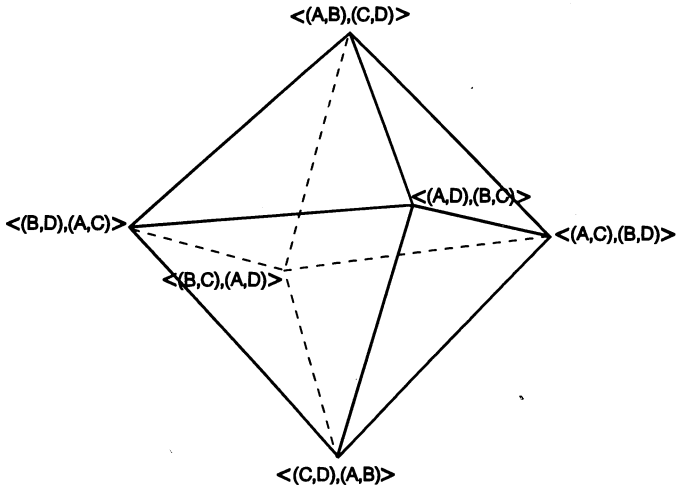

FIG. 10. *Octahedron*.

and $\boldsymbol{\sigma} = (\sigma_1, \ldots, \sigma_n)$ are permutations of N_n. Then, define

$$\rho(a_{\boldsymbol{\pi}}, a_{\boldsymbol{\sigma}}) = \left(\sum_{i=1}^{n} (a_{\pi_i} - a_{\sigma_i})^2 \right)^{1/2}.$$

Critchlow (1985) shows that this extension of Spearman's ρ to partially ranked data is equivalent to the fixed vector metric F_{fv}, which he discusses in detail. The ρ-distance between any two points that differ by the inversion of two consecutive pseudoranks a_i and a_{i+1} is $\rho = \sqrt{2}\,|a_i - a_{i+1}|$. Recall that it is assumed that all observations in the data set are ranked with the same set of pseudoranks. If the pseudoranks are the integers 1 through r, (i.e., $a_{n_1 + \cdots + n_i} = i$, $1 \le i \le r$) then the ρ-distance reduces to $\rho = \sqrt{2}$. In this case, the ρ-distance between all "adjacent" points is constant, and all of the 3-faces are regular Archimedean solids. On the other hand, if the pseudoranks are tied ranks, then the distance between adjacent points is not constant, but it does follow that $\sum_{i=1}^{n} a_i = N(N+1)/2$. The resulting 3-faces are not necessarily regular, but they can be inscribed in a truncated octahedron by placing the vertex corresponding to a partial ranking at the centroid of the set of compatible full rankings. This offers a promising method for visually examining data sets, such as the APA voting data [Diaconis (1989)], that contain both full and partial rankings.

Turning now to Kendall's τ, it follows immediately from the above properties of 1-faces and adjacent vertices that for ordinary full rankings, Kendall's τ is equal to the minimum number of edges (1-faces) that must be traversed to get from one vertex to another. This induces a natural extension of Kendall's τ to pseudoranked data. We define this extension of Kendall's τ to be the minimum number of edges that must be traversed to get from one point to

TABLE 5
Hausdorff metric T^* vs proposed extension of Kendall's τ: Distance from $\langle a,(b,c),d\rangle$

Ordering	T^*	τ
$\langle a,(b,c),d\rangle$	0	0
$\langle a,(b,d),c\rangle$	2	1
$\langle a,(d,c),b\rangle$	2	1
$\langle b,(a,c),d\rangle$	2	1
$\langle b,(a,d),c\rangle$	3	2
$\langle b,(d,c),b\rangle$	4	2
$\langle c,(a,d),b\rangle$	3	2
$\langle c,(a,b),d\rangle$	2	1
$\langle c,(b,d),a\rangle$	4	2
$\langle d,(b,c),a\rangle$	5	3
$\langle d,(a,c),b\rangle$	4	2
$\langle d,(b,a),c\rangle$	4	2

another. This extension trivially satisfies all of the properties of a metric. From Corollary 2 it follows that it is also right invariant; that is, it is invariant under the permutation of item labels. Note that this extension of Kendall's τ depends only on $n_1, n_2, \ldots, n_r$, and not on the actual values of the pseudoranks.

Because it has such appealing graphical properties, this extension of Kendall's τ merits further study, particularly in the context of partially ranked data. As shown in Table 5 for $a_1 < a_2 = a_3 < a_4$, this graphically induced version of Kendall's τ for partially ranked data is different from the Hausdorff extension of Kendall's τ, T^*, that is discussed in detail by Critchlow (1985). It also differs from the "metric" $I(\boldsymbol{\pi}, \boldsymbol{\sigma})$ proposed by Diaconis [(1988), page 127] for partial rankings. Although $I(\boldsymbol{\pi}, \boldsymbol{\sigma})$ has beautiful combinatoric properties, it is not a metric because it is not symmetric in its two arguments. To obtain a counterexample to the symmetry, consider the simplest partial ranking in which $n = 3$, $n_1 = 1$, and $n_2 = 2$; and denote the identity rankings as $id = (1, 2, 2)$. By Theorem 2 of Diaconis [(1988), page 127], it follows that $\Sigma_{\boldsymbol{\eta}} q^{I(id,\boldsymbol{\eta})} = q^2 + q + 1$ where $\boldsymbol{\eta}$ takes the values (1, 2, 2), (2, 1, 2) and (2, 2, 1). This means that there is exactly one point $\boldsymbol{\pi}$, such that $I(id, \boldsymbol{\pi}) = 1$, and one other point $\boldsymbol{\sigma}$, such that $I(id, \boldsymbol{\sigma}) = 2$. Also, by the right invariance of I, there is exactly one point a distance 1 from $\boldsymbol{\pi}$ and one point a distance 2 from $\boldsymbol{\pi}$. If I is symmetric, then $I(id, \boldsymbol{\pi}) = I(\boldsymbol{\pi}, id) = 1$, and $I(\boldsymbol{\pi}, \boldsymbol{\sigma}) = I(\boldsymbol{\sigma}, \boldsymbol{\pi}) = 2$. Hence, there are two points a distance 2 from $\boldsymbol{\sigma}$ which violates the fact that $\Sigma_{\boldsymbol{\eta}} q^{I(h\sigma,\boldsymbol{\eta})} = q^2 + q + 1$.

4. Examples. This section illustrates the application of the results of Section 3 to three data sets that consist of partial rankings with $n > 4$. In particular, Theorem 1 and Corollary 2 are used to determine all of the three dimensional faces of the higher dimensional generalized permutation polytope. Frequently, it is also useful to plot portions of the four-dimensional faces. A permutation polytope in four dimensions is inscribed in a sphere, so it can be

TABLE 6
Data set (n = 5 candidates, A, B, C, D, E; 7 rankers)

Orderings	Rankings
$\langle A, E, (B, C, D)\rangle$	(1, 3, 3, 3, 2)
$\langle A, D, (B, C, E)\rangle$	(1, 3, 3, 2, 3)
$\langle D, A, (B, C, E)\rangle$	(2, 3, 3, 1, 3)
$\langle A, B, (C, D, E)\rangle$	(1, 2, 3, 3, 3)
$\langle B, A, (C, D, E)\rangle$	(2, 1, 3, 3, 3)
$\langle C, B, (A, D, E)\rangle$	(3, 2, 1, 3, 3)
$\langle A, C, (B, D, E)\rangle$	(1, 3, 2, 3, 3)

drawn in three dimensions with distortion just as the surface of a globe or an inscribed truncated octahedron can be drawn as a planar map in two dimensions. This is very similar to the Schlegel diagrams discussed and illustrated by Banchoff (1990).

To determine all of the i-faces most easily in practice, the sequence of pseudoranks is first written down with appropriate equal or less than signs. Then, Theorem 1 is used to determine all of the possible values for $|\omega_k|$, $k = 1, \ldots, n-1$, such that $\omega_1 \subset \omega_2 \subset \cdots \subset \omega_{n-i-1} \subset \omega_{n-i} = N_n$, and such that if $|\omega_j| - |\omega_{j-1}| \geq 2$, then $a_{n-|\omega_{j-1}|} > a_{n-|\omega_j|+1}$. This determines the sizes of the sets Q_k, $k = 1, \ldots, n-1$. Then, for an arbitrary, fixed π, and for each set of possible values of $|Q_k|$, the sets Q_k are written as $\{\pi_{|\omega_{k-1}|+1}, \pi_{|\omega_{k-1}|+2}, \ldots, \pi_{|\omega_k|}\}$, $k = 1, \ldots, n-1$. It then follows from Corollary 2 that the set of vertices of the i-face correspond exactly to the orderings $\langle \pi_n, \pi_{n-1}, \ldots, \pi_1\rangle$ (with parentheses inserted in the required places) such that $Q_k = \{\pi_{|\omega_{k-1}|+1}, \pi_{|\omega_{k-1}|+2}, \ldots, \pi_{|\omega_k|}\}$, $k = 1, \ldots, n-i$. Then, the number of faces are counted by letting π range over S_n.

EXAMPLE 1. In a university department, five job candidates, named A, B, C, D and E, were being evaluated by the seven faculty members to determine which one should be invited for an interview. The chairman asked each faculty member to name a first and second choice. The data are shown in Table 6, both as orderings and as rankings with $a_1 = 1$, $a_2 = 2$, $a_3 = a_4 = a_5 = 3$. In this case, we have $a_1 < a_2 < a_3 = a_4 = a_5$. There are 20 possible partial rankings. The two questions of interest are whether there is a "most popular" candidate to invite and whether there are any "outliers" among the faculty. In determining the 3-faces, it follows from Theorem 1 that the only possible 3-faces occur when $|\omega_1| = 1$ or $|\omega_1| = 4$. It is not possible to have $|\omega_1| = 2$ because $a_5 = a_4$, and it is not possible to have $|\omega_1| = 3$ because $a_5 = a_3$. If either $|\omega_1| = 2$ or $|\omega_1| = 3$, the second condition of Theorem 1 is not satisfied. Hence, for any 3-face we have either $Q_1 = \{\pi_1, \pi_2, \pi_3, \pi_4\}$ and $Q_2 = \{\pi_5\}$, or $Q_1 = \{\pi_1\}$ and $Q_2 = \{\pi_2, \pi_3, \pi_4, \pi_5\}$. In the first case, the orderings of the points on the vertices are $\langle \pi_5, \pi_4, (\pi_3, \pi_2, \pi_1)\rangle$, $\langle \pi_5, \pi_3, (\pi_4, \pi_2, \pi_1)\rangle$, $\langle \pi_5, \pi_2, (\pi_3, \pi_4, \pi_1)\rangle$ and $\langle \pi_5, \pi_1, (\pi_3, \pi_2, \pi_4)\rangle$. The resulting figure is a tetra-

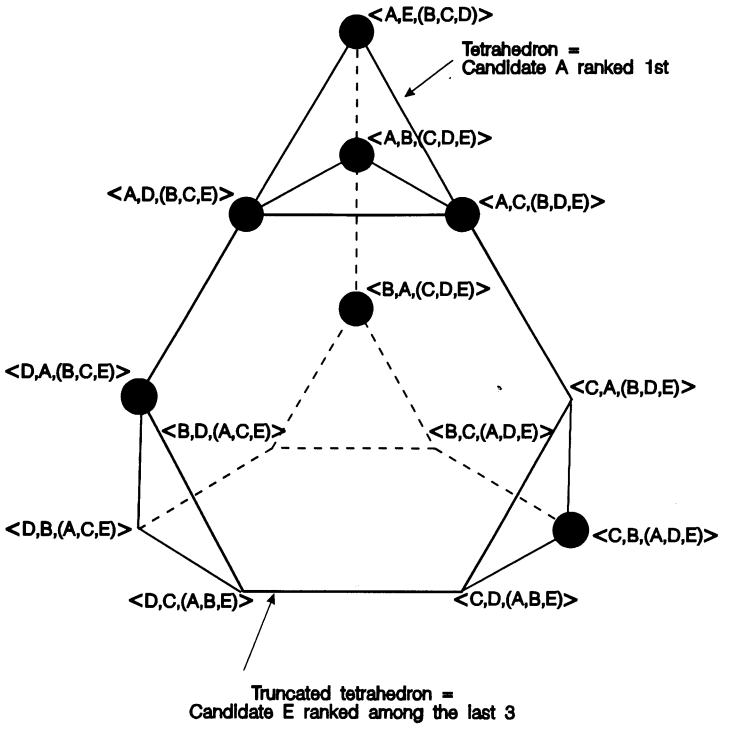

FIG. 11. *Voting data.*

hedron in which all points have the same first choice, and the four vertices correspond to the four possible second choices. There are five different 3-faces that are tetrahedrons, each corresponding to a different first choice. In the second case, that is when $Q_1 = \{\pi_1\}$ and $Q_2 = \{\pi_2, \pi_3, \pi_4, \pi_5\}$, the figure is a truncated tetrahedron in which each vertex has the same candidate ranked among the last three. There are five 3-faces that are tetrahedrons. As shown in Figure 11, all of the data can be graphed by drawing only two adjoining 3-faces, the tetrahedron in which candidate A is ranked first, and the truncated tetrahedron in which candidate E is ranked last. The distances between the points on two different 3-faces of a four-dimensional permutation polytope are somewhat distorted when plotted in three dimensions, but much information is still preserved. It is immediately seen from Figure 11 that candidate A is most popular. Also, there is an outlier (who is, coincidentally, the chairman) at 3, 2, 1, 3, 3. Better intuition about Figure 11 can be obtained by noting that the maximum number of edges that must be traversed to get from any one point to another is 3. That is equivalent to saying that the extension of Kendall's τ proposed in Section 3 takes the values 0, 1, 2 and 3. In fact, each point has four points that are adjacent, six points that are two edges away, and nine points that are three edges away.

TABLE 7
Data set (n = 5 types of crackers; 16 mothers and 22 preschool boys)

Orderings	
Boys	**Mothers**
ACS	CRA
GCA	SRG
ACG	CSA
CAG	CSA
CGA	SRA
ARC	SCR
CSA	SCG
SCR	GAR
AGC	SAR
ARG	CSA
AGC	RSC
ACS	RAG
GRA	SCG
CGA	SAR
ACS	GAS
CGS	SCA
ARC	
ACG	
RAC	
AGC	
ACG	
CAG	

EXAMPLE 2. Table 7 contains the orderings for partially ranked data in which 16 mothers and 22 preschool boys were asked to taste five crackers. A = animal crackers, R = Ritz crackers, S = Saltine crackers, C = cheese crackers and G = Graham crackers. [See Critchlow (1985).] Each mother and preschooler named their first three choices, but did not differentiate between their last two choices. This means that $n = 5$, $r = 4$, $n_1 = 1$, $n_2 = 1$, $n_3 = 1$ and $n_4 = 2$; and the pseudoranks are $a_1 < a_2 < a_3 < a_4 = a_5$. The corresponding generalized permutation polytope, which is inscribed in a sphere in four dimensions, has 60 vertices. When $i = 3$, condition (ii) of Theorem 1 is not satisfied if $|\omega_1| = 2$ because $a_4 = a_5$. It follows that $|\omega_2| = 5$, and there are three different kinds of 3-faces which corresponds to $|\omega_1| = 4$, $|\omega_1| = 3$ and $|\omega_1| = 1$. In terms of the sets Q_k, the three cases are:

(i) $Q_1 = \{\pi_1\pi_2, \pi_3, \pi_4\}$, $Q_2 = \{\pi_5\}$.
(ii) $Q_1 = \{\pi_1\pi_2, \pi_3\}$, $Q_2 = \{\pi_4, \pi_5\}$.
(iii) $Q_1 = \{\pi_1\}$, $Q_2 = \{\pi_2, \pi_3, \pi_4, \pi_5\}$.

In the first case, the 3-face is a truncated tetrahedron corresponding to the cracker labeled π_5 being ranked first. In the second case, the 3-face is a triangular prism. The vertices of the triangular prism are $\langle \pi_5, \pi_4, \pi_3, (\pi_2, \pi_1)\rangle$,

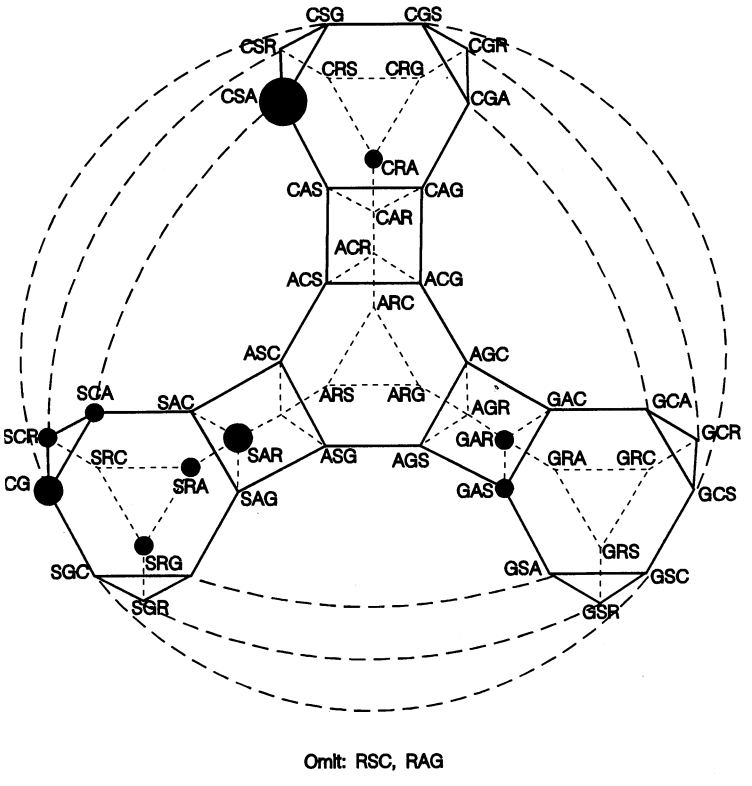

FIG. 12a. *Cracker data: mothers.*

$\langle \pi_5, \pi_4, \pi_1, (\pi_3, \pi_2)\rangle$, $\langle \pi_4, \pi_5, \pi_3, (\pi_2, \pi_1)\rangle$, $\langle \pi_4, \pi_5, \pi_2, (\pi_1, \pi_3)\rangle$, $\langle \pi_4, \pi_5, \pi_1, (\pi_2, \pi_3)\rangle$ and $\langle \pi_5, \pi_4, \pi_2, (\pi_1, \pi_3)\rangle$. In the third case, the 3-face is a truncated octahedron corresponding to the cracker labeled π_1 being ranked among the last. Its three-dimensional faces consist of five truncated octahedrons, five truncated tetrahedrons, and 10 triangular prisms. The maximum number of edges that must be traversed to get from one point to another is six, and each point is adjacent to four other points.

Figures 12a and Figure 12b show plots of the partial rankings for the mothers and boys, respectively, on a portion of the four-dimensional polytope. The differences between the mothers and the boys are readily apparent: The boys tend to prefer animal crackers and the mothers tend to prefer saltines. Because the surface of the polytope in $\mathbb{R}^4$ has been mapped onto $\mathbb{R}^3$, parts of the figure are stretched. Clearly visible in the figures are four truncated tetrahedrons and three triangular prisms. The dashed lines are all of length 1, and form three more triangular prisms. The missing truncated tetrahedron, which has vertices all beginning with R, as well as the other four triangular prisms, are behind the middle of the figure and are not drawn. Only two of the mothers and one of the preschool boys chose partial rankings beginning with R which would be plotted on the omitted truncated tetrahedron. The spaces

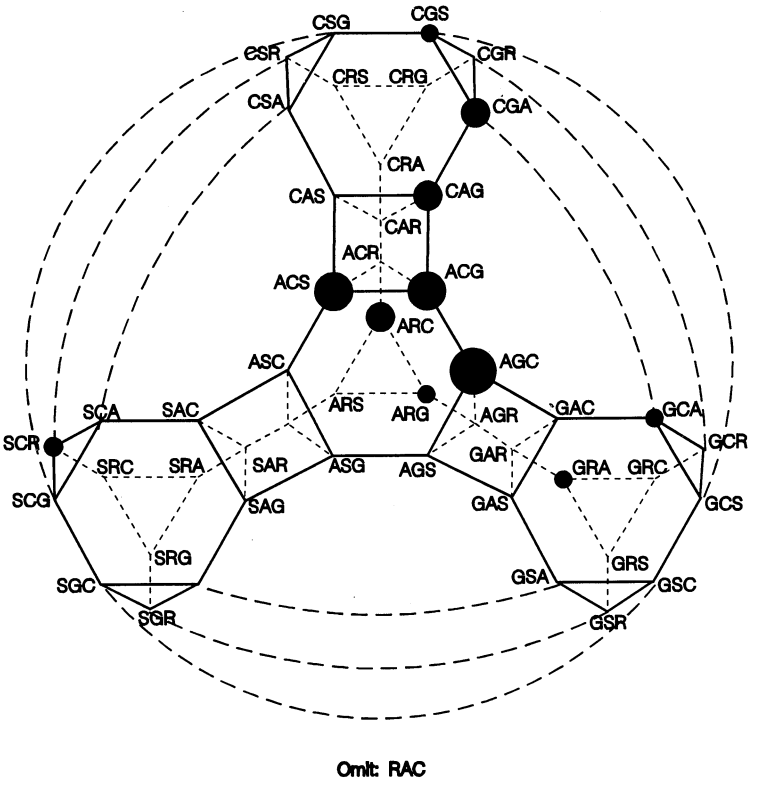

FIG. 12b. *Cracker data: boys.*

between the prisms and the truncated tetrahedrons are filled by the truncated octahedrons. Parts of all five truncated octahedrons can be discerned in the figures, but they are very distorted. This is because more information seems available from the picture if the truncated tetrahedrons are drawn with as little distortion as possible. The truncated octahedrons can be plotted separately, but little additional insight into the data is obtained.

EXAMPLE 3. In a major city, Catholic Charities mailed a survey to a sampling of the members of the local diocese asking each person to rank from 1 to 3 the top three services needed in the community as they saw them. The list of possible choices were:

I = Intensive therapy for emotionally troubled youth and their families

E = Employment assistance for the unemployed

F = Food and financial assistance for families in crisis

L = Legal assistance for immigrants and families

M = Marriage and family counseling

D = Day care for low income families

A = Adoption

O = Outreach to refugees arriving in the city

S = Alcohol and substance abuse treatment for adolescents

P = Prepared meal and health services for low-income senior citizens

H = Housing for low and moderate income families

Table 8 shows the frequencies with which each partial ordering was chosen. Altogether there were 576 respondents to the survey who listed a first, second and third choice; and 284 of the possible 990 partial rankings were chosen.

In this example the pseudoranks are $a_1 < a_2 < a_3 < a_4 = a_5 = a_6 = a_7 = a_8 = a_9 = a_{10} = a_{11}$. The resulting permutation polytope is inscribed in a sphere in $\mathbb{R}^{10}$ and has 990 vertices. Using Theorem 1, it follows that there are four different possibilities for the sizes of ω_k:

(a) $|\omega_k| = 1$, $k = 1, \ldots, 7$; $|\omega_8| = 11$.
(b) $|\omega_k| = 1$, $k = 1, \ldots, 6$; $|\omega_7| = 10$; $|\omega_8| = 11$.
(c) $|\omega_k| = 1$, $k = 1, \ldots, 6$; $|\omega_7| = 9$; $|\omega_8| = 11$.
(d) $|\omega_k| = 1$, $k = 1, \ldots, 5$; $|\omega_6| = 9$; $|\omega_7| = 10$; $|\omega_8| = 11$.

The resulting sets Q_k are

(a) $Q_k = \{\pi_k\}$, $k = 1, \ldots, 7$; $Q_8 = \{\pi_8, \pi_9, \pi_{10}, \pi_{11}\}$.
(b) $Q_k = \{\pi_k\}$, $k = 1, \ldots, 6$; $Q_7 = \{\pi_7, \pi_8, \pi_9, \pi_{10}\}$; $Q_8 = \{\pi_{11}\}$.
(c) $Q_k = \{\pi_k\}$, $k = 1, \ldots, 6$; $Q_7 = \{\pi_7, \pi_8, \pi_9\}$; $Q_8 = \{\pi_{10}, \pi_{11}\}$.
(d) $Q_k = \{\pi_k\}$, $k = 1, \ldots, 5$; $Q_6 = \{\pi_6, \pi_7, \pi_8, \pi_9\}$; $Q_7 = \{\pi_{10}\}$; $Q_8 = \{\pi_{11}\}$.

In the first case, the 3-face is a truncated octahedron in which items labeled π_1 through π_7 are ranked among the last eight, and the remaining four items are permuted among the first, second, third and fourth places. In the second case, the 3-face is a truncated tetrahedron in which item π_{11} is ranked first, and items π_7, π_8, π_9 and π_{10} are permuted among second, third and two fourth places. In the third case, the 3-face is a triangular prism in which items π_{10} and π_{11} are permuted between first and second place, and π_7, π_8, and π_9 are permuted among the third and two of the fourth places. And in the fourth case, the 3-face is a tetrahedron in which item π_{11} is ranked first, item π_{12} is ranked second, and items π_6, π_7, π_8 and π_9 are permuted among the third and three of the fourth places. Altogether, the 3-faces consist of 330 truncated octahedrons, 2310 truncated tetrahedrons, 4620 triangular prisms and 13,860 tetrahedrons.

In spite of the large number of 3-faces, a great deal of the data can be illustrated by choosing the 3- and 4-faces that contain the largest percentage of the data. For example, if interest is restricted to any five items, then the points can be plotted on the same type of figure used in Example 2. This is done in Figure 13 for F, E, D, H and P. The truncated tetrahedron corresponding to rankings beginning with P is hidden behind the figure. This hidden truncated

TABLE 8
Data set (n = 11 choices; 576 survey respondents)

ADH	1	DSI	1	FDP	2	FPS	7	IEP	3	MID	1	PME	3
ADS	1	DSM	2	FDS	1	FSD	1	IES	2	MIE	1	PMF	1
AED	1	EAF	1	FEA	1	FSE	1	IFO	1	MIF	3	PMO	1
AEF	1	EDF	3	FED	10	FSH	1	IFS	2	MIL	1	SAD	2
AEL	1	EDH	3	FEH	11	FSI	2	IMA	1	MIO	1	SAE	1
AEO	1	EDM	2	FEI	6	FSL	1	IMD	1	MIS	3	SDE	2
AFP	2	EDP	3	FEM	6	FSM	1	IMF	1	MLA	1	SDF	1
AHS	1	EFA	2	FEP	10	FSO	2	IML	1	MPA	2	SDI	1
AIS	1	EFD	4	FES	2	FSP	4	IMP	2	MPF	2	SED	2
ALH	1	EFH	5	FHD	9	HAD	1	IMS	4	MSE	3	SEF	1
AMI	1	EFI	2	FHE	10	HDE	2	IOA	1	MSF	1	SEL	1
APD	1	EFL	2	FHI	2	HDF	2	IPD	1	OFE	1	SEP	2
APM	1	EFM	3	FHM	2	HDI	3	IPE	1	OIS	1	SFD	2
ASM	1	EFO	1	FHO	2	HDL	1	IPF	2	OLF	1	SFE	2
DAL	1	EFP	4	FHP	9	HDM	2	IPH	1	OME	1	SFH	1
DAS	1	EFS	1	FHS	4	HDO	1	IPM	1	OMF	1	SFI	3
DEH	2	EHD	2	FIE	4	HDP	2	IPO	1	OPF	1	SFL	1
DEP	1	EHF	2	FIH	2	HDS	1	ISD	2	OPL	1	SFM	1
DFE	2	EHI	1	FIP	1	HED	2	ISE	1	PAF	3	SFP	2
DFH	2	EHL	1	FIS	3	HEF	1	ISF	1	PDE	1	SHE	2
DFI	1	EIF	2	FLH	1	HEP	1	ISM	3	PDF	2	SHL	1
DFM	1	ELA	1	FLS	1	HFD	1	ISP	1	PDI	2	SHP	1
DFO	1	ELI	1	FMA	1	HFE	9	LMD	1	PDL	1	SIA	1
DFP	2	EMS	1	FMD	2	HFM	1	MAD	2	PED	2	SIF	3
DFS	1	EPF	2	FME	1	HFO	1	MAE	2	PEF	2	SIH	1
DHE	1	EPH	1	FMH	1	HFP	6	MAI	1	PEI	1	SIL	1
DHF	3	EPM	2	FMI	1	HFS	2	MAP	1	PEM	1	SIM	3
DHO	1	ESH	1	FML	1	HIE	1	MAS	1	PFA	2	SIP	5
DHP	2	ESI	1	FMP	1	HLA	1	MDP	2	PFD	5	SLE	1
DIF	1	ESM	1	FMS	2	HOF	1	MED	1	PFE	7	SMD	1
DIP	1	ESP	3	FOD	2	HPF	3	MEF	1	PFH	4	SME	1
DMF	1	FAD	1	FOE	2	HPI	4	MEH	1	PFI	1	SMP	1
DMI	1	FAM	2	FOL	1	HPL	1	MEP	1	PFL	1	SOD	1
DMS	1	FAP	2	FOP	1	HPS	1	MFA	1	PFO	1	SPE	4
DOI	1	FAS	1	FPA	2	HSE	1	MFE	2	PFS	6	SPF	1
DPF	4	FDA	1	FPD	11	HSP	1	MFH	3	PHD	1	SPH	1
DPH	1	FDE	9	FPE	7	IAS	1	MFI	2	PHF	3	SPM	1
DPM	2	FDH	2	FPH	12	IDE	1	MFL	1	PHS	2	SPO	1
DPS	2	FDI	3	FPI	5	IDS	1	MFP	2	PID	1		
DSE	1	FDL	1	FPM	1	IED	1	MFS	2	PIE	1		
DSH	1	FDM	2	FPO	5	IEF	2	MHE	1	PIF	1		

No other orderings were chosen.

tetrahedron is shown at the bottom of Figure 13. The most striking feature of the 4-face in Figure 13 is that although it contains only 20 of the 21,120 possible 3-faces, it contains almost 1/3 of the data. And the truncated tetrahedron in Figure 13 in which F is ranked first contains 92 responses or 16 percent of the data. Also interesting is the fact that the points on this truncated tetrahedron are chosen almost uniformly except for *FDH* and *FDP*.

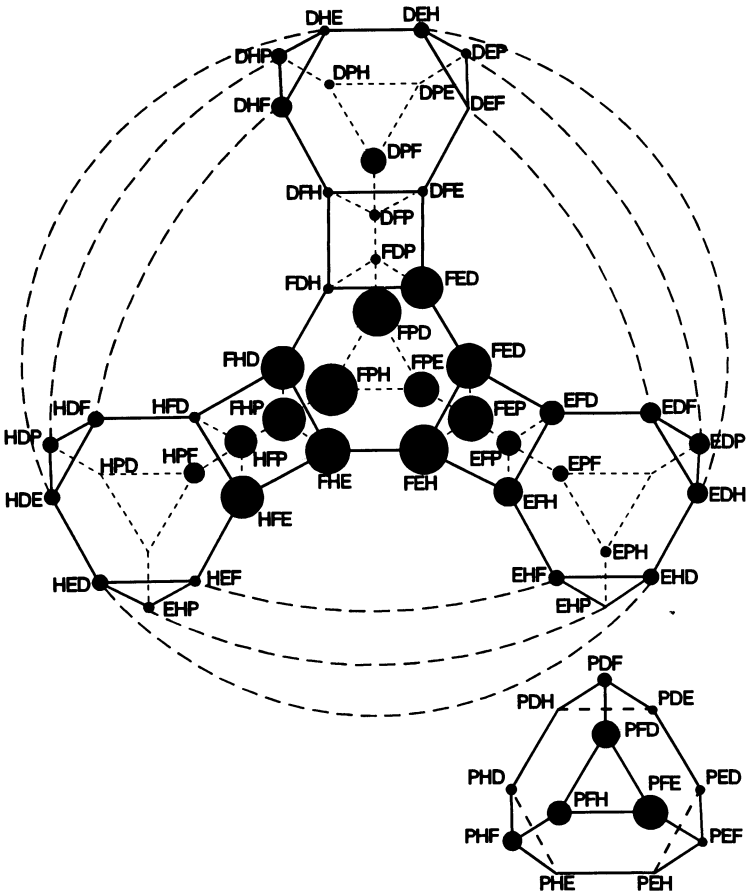

FIG. 13. *Catholic charities data.*

The frequency distributions on the other four truncated tetrahedrons in Figure 13 are all fairly similar to each other, but overall their frequencies are considerably less than those of the truncated tetrahedron beginning with F. These observations are useful in guiding the choice of a metric based model for the data.

Faces can also be chosen to answer specific questions of interest. In this case, there is interest in the relationship between I and S. Figure 14a contains a truncated octahedron whose vertices correspond to the partial rankings in which the first, second and third choices are chosen from F, P, S and I. On the right-hand side of the figure, S precedes I; on the left-hand side, I precedes S. Clearly, S precedes I more frequently on this particular 3-face. As a contrast, Figure 14b contains a hexagon with all of the permutations of S, I and M. In this case, I precedes S. These observations were interpreted in light of the qualitative differences between the choices F and P,

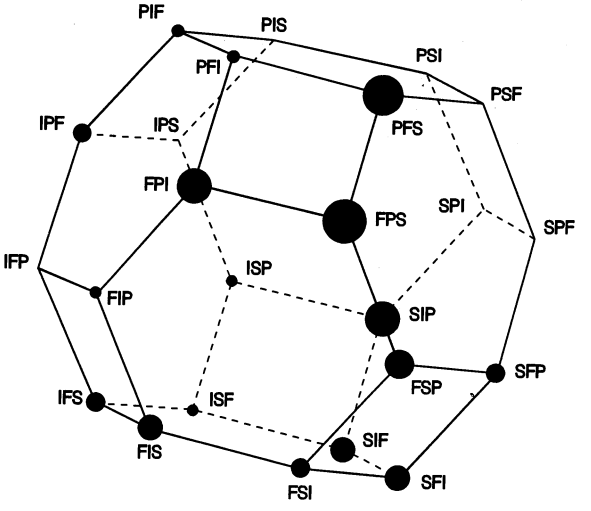

FIG. 14a. *Catholic charities data.*

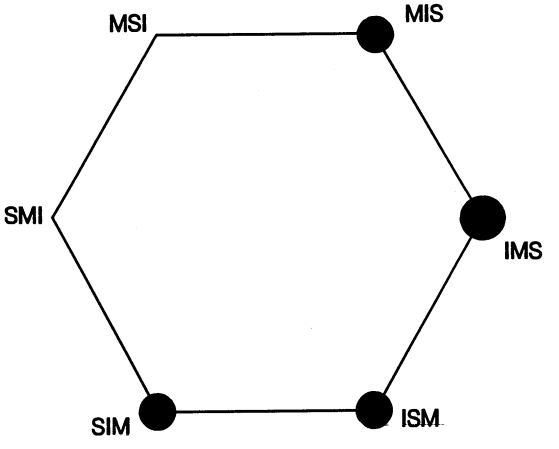

FIG. 14b. *Catholic charities data.*

and the choice M. Other faces to illustrate the relationship between S and I contained too few points to be of interest.

5. Proofs.

PROOF OF THEOREM 1. First, we prove that the system of (4) and (5) determines an i-dimensional face when conditions (i) and (ii) hold. Clearly, the points satisfying (4) and (5) are a subset of the points satisfying (2) and (3) in the definition of the permutation polytope. Because the system is consistent, it

determines a face. The rank of the system is $n - i$. To show that the face is of dimension i, we use Proposition 4.3 of YKK, page 36, and show that the system has exactly $n - i$ linearly independent constraints. To do this, let ω be any subset of N_n, and define $Q_k = \omega_k/\omega_{k-1}$ for $1 \le k \le n - i$. If ω is the union of the elements in some subset of $\{Q_k;\ 1 \le k \le n - i\}$, then the $n - i$ constraints in (5) imply

$$\sum_{j \in \omega} x_j = \sum_{j=1}^{|\omega|} a_{n-j+1}.$$

On the other hand, if ω is not the union of the elements in any subset of $\{Q_k;\ 1 \le k \le n - i\}$, then it is sufficient to show that there is a solution to (4) and (5) such that

$$\sum_{i \in \omega} x_i < \sum_{i=1}^{|\omega|} a_{n-i+1}. \tag{7}$$

Let p be the largest integer such that $\omega_p \not\subset \omega$ and $\omega_{p+1} \not\subset \omega$; and let q be the smallest integer such that $\omega \not\subset \omega_q$ and $\omega \not\subset \omega_{q-1}$. If $|Q_k| = 1$ for all integers k such that $p < k \le q$, then ω is the union of the elements in some subset of $\{Q_k;\ 1 \le k \le n - i\}$. Hence, we must have that $|Q_{k'}| \ge 2$ for some integer k' where $p < k' \le q$. This implies that $a_{n-|\omega_{k'}|+1} < a_{n-|\omega_{k'-1}|}$. Now consider the solution defined by letting $x_j = a_{n-j+1}$ for $j \in N_n \setminus Q_{k'}$ and $x_j = (\Sigma_{s \in Q_{k'}} a_{n-s+1})/|Q_{k'}|$ for $j \in Q_{k'}$. Clearly this solution satisfies (5). Because the a_j's are nondecreasing, the solution satisfies (4). And because $\omega_k \setminus \omega$ is nonempty and the a_j's are nondecreasing, the solution satisfies (7). Hence, the face has dimension i.

Conversely, suppose that we have an i-face of the permutation polytope satisfying (4) and (5). Without loss of generality, assume that $|\omega_j| < |\omega_k|$ implies $j < k$, $j, k = 1, 2, \ldots, n - i$. Assume that condition (ii) does not hold so that for some integer j we have $|\omega_j \Delta \omega_{j-1}| \ge 2$ and $a_{n-|\omega_j|+1} = a_{n-|\omega_{j-1}|}$. Straightforward calculations show that the system in (4) and (5) is equivalent to the system defined by (4) and (5) augmented with

$$\sum_{j \in \omega_k} x_j = \sum_{j=1}^{|\omega_*|} a_{n-j+1},$$

where $\omega_* = \omega_{j-1} \cup \{x_*\}$, where $x_* \in Q_j$. Hence, the face is of dimension less than i which is a contradiction. Next, suppose that the inclusions in condition (i) of the theorem do not hold. Then there is a pair of sets, ω_p and ω_q, such that neither is a subset of the other. Without loss of generality, we can assume that $p = q - 1$ and that $|\omega_p| \le |\omega_q|$. Then for any point x on the i-face, we have

$$\sum_{j \in \omega_p} x_j + \sum_{j \in \omega_q} x_j = \sum_{j=1}^{|\omega_p|} a_{n-j+1} + \sum_{j=1}^{|\omega_q|} a_{n-j+1}$$

$$= \sum_{j \in \omega_p \cup \omega_q} x_j + \sum_{j \in \omega_p \cap \omega_q} x_j \le \sum_{j=1}^{|\omega_p \cup \omega_q|} a_{n-j+1} + \sum_{j=1}^{|\omega_p \cap \omega_q|} a_{n-j+1}.$$

Because neither ω_q or ω_p is a subset of the other, we have that $|\omega_p \Delta \omega_q| \geq 2$, which in turn implies that $a_{n-|\omega_q|+1} < a_{n-|\omega_p|}$. Because the pseudoranks are nondecreasing, it follows that

$$\sum_{j=1}^{|\omega_p \cup \omega_q|} a_{n-j+1} + \sum_{j=1}^{|\omega_p \cap \omega_q|} a_{n-j+1} < \sum_{j=1}^{|\omega_q|} a_{n-j+1} + \sum_{j=1}^{|\omega_p|} a_{n-j+1}.$$

This contradiction implies that the inclusions in condition (i) must hold. □

PROOF OF COROLLARY 2. The proof of Corollary 2 is aided by the following definitions involving multisets. The multiset corresponding to the pseudoranks in (1) is $\{w_1^{n_1}, w_2^{n_2}, \ldots, w_r^{n_r}\}$, where $w_1 < w_2 < \cdots < w_r$ are the r distinct values of the pseudoranks, and w_i occurs n_i times. The set of $\binom{n}{n_1 \quad n_2 \quad n_3 \quad \cdots \quad n_r}$ distinct permutations of the multiset $\{1^{n_1}, 2^{n_2}, \ldots, r^{n_r}\}$ is denoted by $\mathfrak{G}$, and a permutation of (nondistinct) pseudoranks is denoted by $w_\sigma = (w_{\sigma_1}, w_{\sigma_2}, \ldots, w_{\sigma_n})$, where $\sigma \in \mathfrak{G}$. Define the set $A(\sigma) = \{\pi \in S_n$ such that $w_\sigma = a_{\pi^{-1}}\}$. Note that π is in $A(\sigma)$ if and only if $x_{\pi_k} = a_k$ is equivalent to $x_k = w_{\sigma_k}$. Define the pseudoinverse of $\pi \in S_n$ to be the element $\sigma \in \mathfrak{G}$ such that $\pi \in A(\sigma)$. This pseudoinverse is unique and well defined, but more thanone element of S_n can have the same pseudoinverse. Next, for any i-face, define $S(Q_1, Q_2, \ldots, Q_{n-i})$ to be the set of all possible permutations $\pi \in S_n$ such that $Q_k = \{\pi_{|\omega_{k-1}|+1}, \pi_{|\omega_{k-1}|+2}, \ldots, \pi_{|\omega_k|}\}$, and define $S^{-1}(Q_1, Q_2, \ldots, Q_{n-i})$ to be the set of pseudoinverses of the permutations $(\pi_n, \pi_{n-1}, \ldots, \pi_1)$, where $\pi \in S(Q_1, Q_2, \ldots, Q_{n-i})$.

Now, suppose that w_σ is a vertex such that $\sigma \in S^{-1}(Q_1, Q_2, \ldots, Q_{n-i})$ and let $x = w_\sigma$. By definition of $S^{-1}(Q_1, Q_2, \ldots, Q_{n-i})$, we have $x_{\pi_k} = a_{n-k+1}$, $k = 1, 2, \ldots, n$ where $\pi \in S(Q_1, Q_2, \ldots, Q_{n-i})$. Hence,

$$\sum_{j \in Q_k} x_j = \sum_{j=j_k}^{|Q_k|} x_{\pi_j} = \sum_{j=j_k}^{|Q_k|} a_{n-j+1} \quad \text{for } k = 1, 2, \ldots, n-i, \tag{8}$$

where $j_k = |\omega_{k-1}| + 1$. This shows that a_σ is on the face determined by $Q_1, Q_2, \ldots, Q_{n-i}$. Conversely, suppose that w_η is not on the face generated by $Q_1, Q_2, \ldots, Q_{n-i}$; that is, $\eta \notin S^{-1}(Q_1, Q_2, \ldots, Q_{n-i})$. Let $\mathbf{x} = w_\eta$. Then, because a_{n-j+1} is decreasing in j, (8) holds at $\mathbf{x} = w_\eta$ only if $\{x_{\pi_{j_k}}, x_{\pi_{j_k+1}}, \ldots, x_{\pi_{|Q_k|}}\} = \{a_{n-j_k+1}, a_{n-j_k+2}, \ldots, a_{n-|Q_k|+1}\}$ for each $k = 1, 2, \ldots, n-i$. This implies that $\eta \in S^{-1}(Q_1, Q_2, \ldots, Q_{n-i})$, which is a contradiction. The corollary follows immediately by noting that the ordering corresponding to any pseudoranking can be obtained by simply inserting the proper notation into any element of $A(\sigma)$. □

Acknowledgments. The author thanks Pat Gerard for his computational help. The author appreciates the efforts of the referees; their efforts led to an improved paper. And the author is especially grateful to Vijay Nair, Robert Serfling and Yuly Koshevnik for their many helpful suggestions and comments.

REFERENCES

BABA, Y. (1986). Graphical analysis of rank data. *Behaviormetrika* **19** 1–15.

BABA, Y. (1988). Graphical analysis of ranks. In *Recent Developments in Clustering and Data Analysis* (C. Hayashi, E. Diday, M. Jambo and N. Ohsumi, eds.) 87–96. Academic, New York.

BANCHOFF, T. F. (1990). *Beyond the Third Dimension*. Scientific American Library, New York.

CLEVELAND, W. S. (1985). *The Elements of Graphing Data*. Wadsworth Advanced Books and Software, Monterey.

COHEN, A. (1990). Data analysis of full and partial rankings. Technical Report, Dept. Industrial Engineering and Management, Technion-Israel Institute of Technology, Haifa, Israel.

COHEN, A. and MALLOWS, C. (1980). Analysis of ranking data. Technical memorandum, Bell Laboratories, Murray Hill, NJ.

CRITCHLOW, D. E. (1985). *Metric Methods for Analyzing Partially Ranked Data. Lecture Notes in Statist.* **34**. Springer, New York.

CRITCHLOW, D. E. and VERDUCCI, J. S. (1989). Detecting a trend in paired rankings. Technical Report 418, Dept. Statistics, Ohio State Univ.

DIACONIS, P. (1988). *Group Representations in Probability and Statistics*. IMS, Hayward, CA.

DIACONIS, P. (1989). A generalization of spectral analysis with application to ranked data. *Ann. Statist.* **17** 949–979.

DUNCAN, O. D. and BRODY, C. (1982). Analyzing n rankings of three items. In *Social Structure and Behavior* (R. M. Hansen D. Mechanic, A. O. Haller. and T. S. Hauser, eds.) 269–309. Academic, New York.

KNUTH, D. (1981). *The Art of Computer Programming* **2**, 2nd ed. Addison-Wesley, Reading, MA.

MCCULLAGH, P. (1990). Models on spheres and models for permutations. *Probability Models and Statistical Analyses for Ranking Data. Lecture Notes in Statist.* **80** 278–283. Springer, New York.

MCCULLAGH, P. and YE, J. (1993). Matched pairs and ranked data. *Probability Models and Statistical Analyses for Ranking Data* (M. A. Fligner and J. S. Verducci, eds.). *Lecture Notes in Statist.* **80** 299–306. Springer, New York.

SCHULMAN, R. S. (1979). A geometric model of rank correlation. *Amer. Statist.* **33** 77–80.

STANLEY, R. (1985). *Enumerative Combinatorics*. Wadsworth, Belmont, CA.

THOMPSON, G. L. (1993). Graphical techniques for ranked data. *Probability Models and Statistical Analyses for Ranking Data Lecture Notes in Statist.* **80**. 294–298 Springer, New York.

YEMELICHEV, V. A., KOVALEV, M. M. and KRAVTSOV, M. K. (1984). *Polytopes, Graphs, and Optimisation*. Cambridge Univ. Press.

DEPARTMENT OF STATISTICAL SCIENCE
SOUTHERN METHODIST UNIVERSITY
DALLAS, TEXAS 75275-0332